

PROGRESS IN SEMITRANSSPARENT CRYSTALLINE SILICON SOLAR CELLS

A. Boueke, R. Kühn, M. Wibrall, P. Fath, G. Willeke, E. Bucher

Universität Konstanz, Fakultät für Physik, P.O. Box X916, D-78457 Konstanz, Germany

Tel.: 0049-7531-88-2088, Fax: 0049-7531-88-3895

email: arnd.boueke@uni-konstanz.de

ABSTRACT: The first semitransparent crystalline silicon solar cells on CZ-silicon are presented. The realisation is based on the POWER solar cell design [1], whereby perpendicularly overlapping grooves on front and back side lead to holes of variable diameter. The grooves themselves are formed in the silicon using a dicing saw. The presented investigations compare three different approaches of semitransparent silicon solar cells with transmittances of around 18%. The solar cell manufacturing process was kept as simple as possible. Only six different steps were necessary to produce semitransparent silicon solar cells (including a single ARC), leading to a cell efficiency close to 10%. The influence of three different cell designs on the parameters I_{SC} , V_{OC} , FF and cell efficiency is discussed and a comparison of the short circuit current between conventional flat solar cells and semitransparent solar cells at different angles of the incident light is given.

Keywords: semitransparent-1: texturisation-2: silicon-3

INTRODUCTION

In order to find new applications for crystalline silicon solar cells, a novel semitransparent cell design has been developed. These first semitransparent crystalline silicon solar cells open new markets that were previously closed to this technology. In the presented work examples of three different geometrical designs and a very simple process that is compatible with industrial production are presented. The physical properties of these semitransparent crystalline silicon solar cells with a transmittance of around 18% are discussed.

THE SEMITRANSSPARENT SI SOLAR CELL

As for the Power-Solar-Cell [1], [2], [3] the semitransparency of the presented cells is obtained by structuring the silicon wafer with grooves on both sides that are perpendicular to each other.

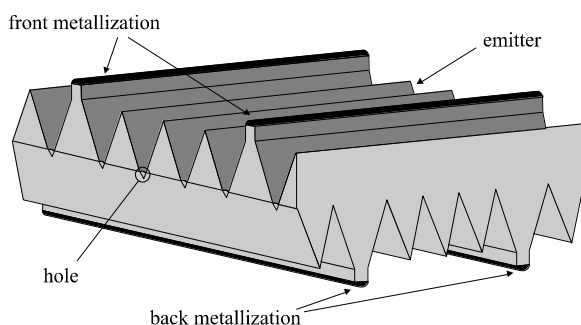


FIG. 1: Schematic presentation of the proposed solar cell structure. By using different types of dicing blades (bevelled or rectangular) the size of the holes and the structure and size of the surfaces may be varied.

Three different cell designs as presented in the following were investigated (see Figs. 1-3). They are distinguished by a varying cell geometry which is obtained by using different dicing blades or by simply changing the dicing parameters. The aim of this study was to clearly reveal the advantage and disadvantages of these cell structures within an industrially compatible solar cell process.

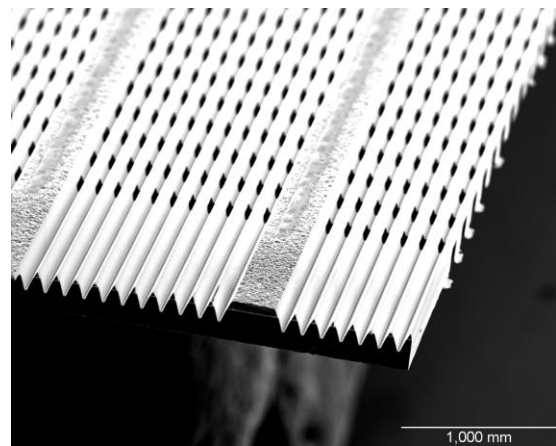


FIG. 2: Type A. The front side is structured with V-grooves. To achieve a transmittance of 16.2 % a rectangular blade was used at the rear side to produce the required larger holes.

The transmittance of these three structures varies between 16.2 % and 18.6 %. The front side of type A (see Fig. 2) was structured with a bevelled blade. This structure provides excellent anti-reflection properties. For the structuring of the rear grooves a rectangular blade was used.

Type B and type C were structured with a rectangular dicing blade on both sides. Nevertheless the obtained cell-designs vary considerably from each other. The front side of type B shows flat plateaus of 120 μm width between two grooves (Fig. 3). The holes and flat plateaus of type C are enormously enlarged as can be seen in Fig.4. The reflection is therefore comparable with the one of flat cells.

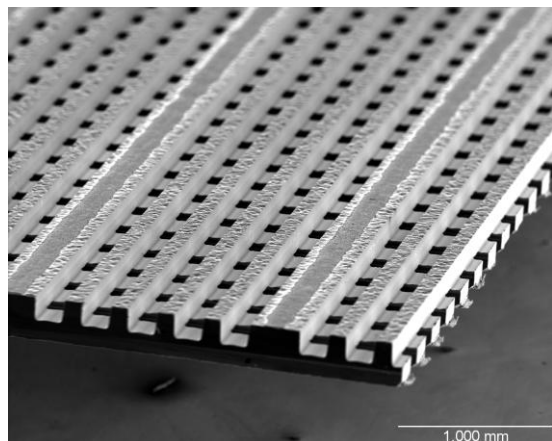


FIG. 3: Type B. Both sides are structured with a rectangular dicing blade. The small plateaus between the grooves are 120 μm wide. The screen printed front metallization can be seen on the larger plateaus.

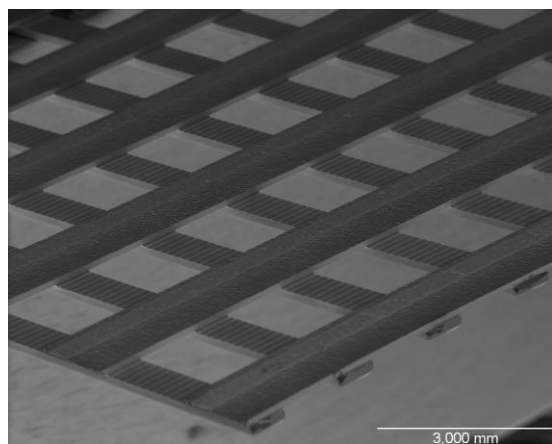


FIG. 4: Type C. By abrasion of large areas on both sides of the wafer holes in the mm-range have been created.

PROCESSING

A very simple process was developed to fabricate semitransparent monofacial crystalline silicon solar cells which is suitable for a low cost industrial solar cell manufacturing environment. In the present study CZ-silicon of 1 Ωcm resistivity was used as base material. Before structuring the wafers were thinned to a thickness of 310 μm . The structuring including hole formation was done using a conventional dicing saw equipped with rectangular or bevelled saw blades. If high throughput is required multiblade or structuring wheel texturisation can be applied. An emitter with a $R_{\text{Sheet}} = 28 \Omega/\text{sqr.}$ was diffused. A PECVD Si nitride was deposited as an antireflection coating.

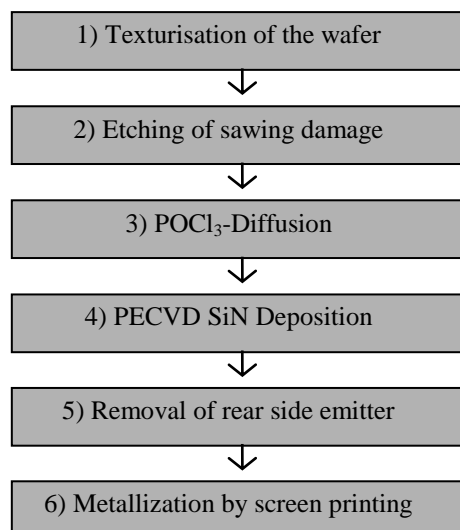


FIG. 5: Process sequence. Only six different steps are necessary to produce semitransparent crystalline solar cells including a PECVD SiN ARC.

In a subsequent step the n-type layer at the cell rear side was removed by applying a very simple technique. Finally the front grid was fired through the SiN ARC layer. It should be notified that the presented novel semitransparent cell designs could be manufactured with a solar cell process and techniques, which are almost identical to the one used in PV industry for conventional solar cells.

Due to the required mechanical stability and different grid designs on the rear side, it was not possible to create three different designs with exactly the same transmittance. Therefore T varies by 2.4%, with values of $T=16.2\%$ for type A, $T=18.2\%$ for type B and $T=18.6\%$ for type C.

OPTICAL PROPERTIES OF THE DIFFERENT DESIGNS

In Fig.6 the spectral dependence of the total hemispherical reflectance is shown for the differently structured cell variants. All three samples are covered by a single anti-reflection coating. The reflectances were measured on single side mechanically structured cells. Measurements on semitransparent cells would result in deviations because it is not possible to focus the small light beam of the used apparatus with a defined ratio of structured and non-structured regions on the cells especially of cell type C. The coverage of the front grid is 6.3% in all three devices and the reflection of the grid is included.

The average reflectance of type A is only $R_{\text{av}} = 10.5\%$ between 400nm and 1100nm. Due to the enhanced light trapping of double-side structured cells, an additional reduction of the reflection in the long wavelength range can be expected for semitransparent cells of type A.

The active areas of cell types B and C have higher average reflectances ($R_{\text{av}}(\text{type B})=16.2\%$, $R_{\text{av}}(\text{type C})=18.3\%$) caused by the non-optimal reflection properties of the rectangular grooves. Especially the light trapping of long wavelength photons is reduced due to the flat plateaus on the front side.

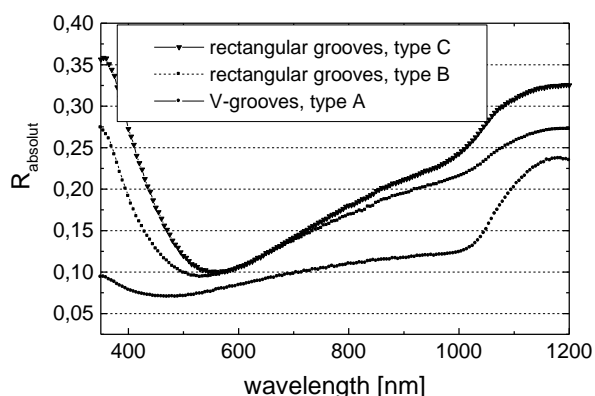


FIG. 6: Total reflectance R as a function of the wavelength for the three cell designs.

SOLAR CELL RESULTS

Prior to this study investigations concerning the grid design, the screen printing above structured regions and the depths of the grooves on the front- and the rear side had to be done to avoid rather low fill factors with series resistances larger than 5 Ohmcm^2 and shunt resistances lower than 150 Ohmcm^2 as observed for first experimental devices.

It was possible to produce $5 \times 5 \text{ cm}^2$ semitransparent monofacial silicon solar cells with a transmittance of 18.2% and a cell efficiency of $\eta = 9.4\%$ (type B). This is about a factor of five larger than the efficiency of semitransparent amorphous silicon solar panels (transmittance $< 5\%$) which have been the only existing semitransparent photovoltaic devices so far.

The solar cell design with deep V-grooves (type A) causes mechanical stability problems and is therefore not easy to realise. Due to the very small size of the holes a large amount of grooves had to be prepared in order to reach the desired transmittance close to 18%. This leads to large areas of unpassivated surfaces and an increasing length of p-n junctions bordering the surface in the holes.

Cell type (Transmittance T)	J_{SC} [mA/cm ²]	V_{OC} [mV]	FF [%]	η [%]
convent. flat cell	27.9	602	76.7	12.9
A (T=16.2%)	25.3	490	65.2	8.1
B (T=18.2%)	25.4	540	69.0	9.4
C (T=18.6%)	20.1	560	70.1	7.8

TAB. 1: Values for J_{SC} , V_{OC} , FF and cell efficiency for the best cells of the three different cell designs. The average

values for the cell efficiency were around 0.3% absolute lower than the above mentioned values.

Both effects decrease the open circuit voltage ($V_{OC(A)} = 490 \text{ mV}$). The spectral response in the long wavelength range (see Fig. 7) is affected by the large size of unpassivated surfaces at the rear side, resulting in J_{SC} of only 25.3 mA/cm^2 , in spite of the good antireflection properties.

Furthermore we believe that the enlarged total length of the p-n junctions that lies in a region of high surface recombination may cause a decrease of the fill factor. This aspect of semitransparent silicon solar cells is presently investigated at the University of Konstanz [4].

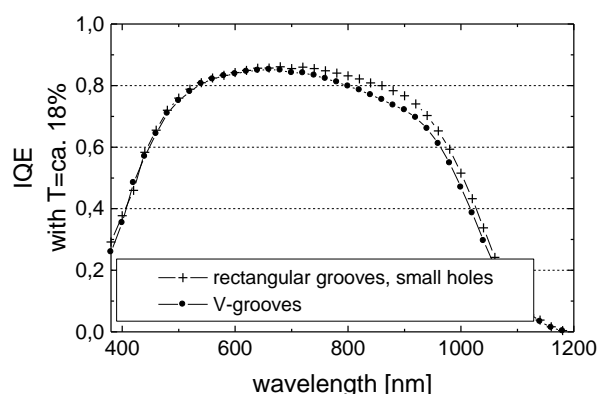


FIG. 7: Absolute IQE of type A and B. The large holes of type C prevent a reliable measurement of IQE. It was not possible to focus the small monochromatic light beam of the used setup on the cell with a defined ratio of structured and unstructured regions.

The cell design with rectangular grooves on both sides and small holes (typeB) shows by far the best results. In spite of 18.2% transmittance J_{SC} is only reduced by 9.2% compared with conventional flat cells, caused by the good antireflection properties of this design (see Fig.6). There is again a strong decrease of V_{OC} caused by the above mentioned damages on the rear side of the solar cell.

The dark I-V-measurements show that these semitransparent silicon solar cells are dominated by the second diode (Fig. 8). Design B has got 14040 small holes compared with 34500 tiny holes of type A. The different amount of holes/cm² of the two cell designs leads to the following dark currents in the space charge regions (fitted with [5]): $I_{02(A)} = 1.6 \cdot 10^{-6} \text{ A/cm}^2$ and $I_{02(B)} = 6.1 \cdot 10^{-7} \text{ A/cm}^2$, which explains the large difference in V_{OC} :

$$\Delta V_{OC} \approx 2K_B T/q \ln a = -48 \text{ mV}$$

$$\text{with } a = I_{02(B)} / I_{02(A)} = 0.38$$

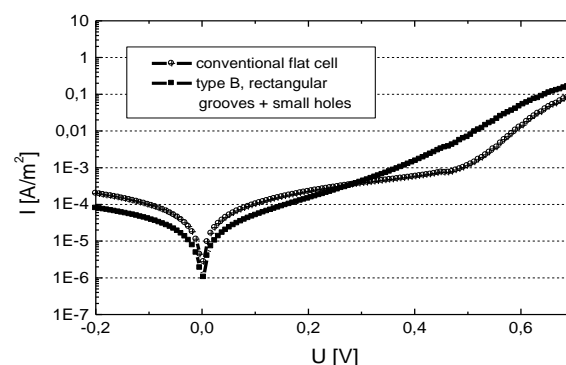


FIG. 8: Dark I-V-characteristic of a conventional flat solar cell and a semitransparent solar cell of type B. Fits with the 1-diode-model give a diode ideality factor ≈ 2 for type B.

For the cells of type C a short circuit current similar to the I_{SC} of conventional flat cell minus 18.6% transmittance, would have been expected. This would result in a $I_{SC}=22.5\text{mA}/\text{cm}^2$. In contrast to that, the measured current was only $I_{SC}=20.1\text{mA}/\text{cm}^2$. The abrasion of bulk volumes during the mechanical texturisation step of these cells led to an effective average thickness of only $151\ \mu\text{m}$ ($d_{\text{aver.}}(\text{type B})=196\ \mu\text{m}$) which reduces the absorption of light and therefore also the short circuit current.

The semitransparent crystalline silicon solar cells are especially suitable for solar architecture (building facades, light gardens, etc.) and for glass sliding roofs within the automobile industry. For those applications it is usually not possible to direct the solar cell towards the sun during at all times. It is therefore important that the solar cell efficiently converts also light that impinges the panel under different angles α than at perpendicular incidence.

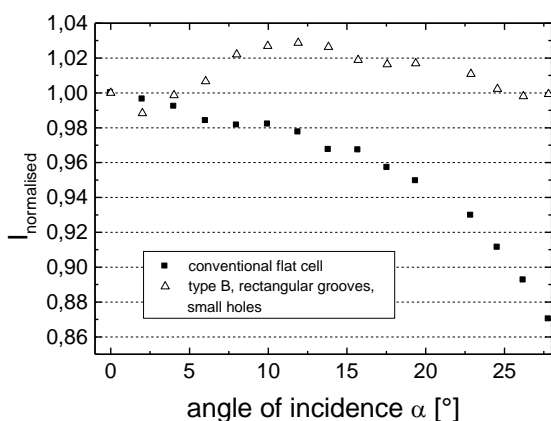


FIG.9: Comparison between currents of rectangularly textured (type B) and flat surfaces as a function of the incidence angle of the impinging light. The currents were normalised by the current at normal incidence ($\alpha=0^\circ$). The direction of the in-coming light was perpendicular to the grooves of type B.

These data were measured on a sunny day on the roof of our laboratory in Konstanz, Germany. The results clearly demonstrate that rectangularly textured surfaces show a superior angular response than flat cells. Due to the decreasing transmittance under non-normal incidence there is even an increase in the short circuit current of the semitransparent cells. For an incidence angle of 25° there is still no loss of I_{SC} for semitransparent cells of type B with a corresponding drop of 10% for flat solar cells.

FUTURE WORK AND CONCLUSION

Future investigations will be mainly focussed on the surface passivation in the rear side grooves.

Simulations with *Dessis*TM [6] showed that more heavily doped Si material is beneficial for these semitransparent Si solar cells. First experiments led already to a cell efficiency of $\eta=9.7\%$ for a $0.5\ \Omega\text{cm}$ wafer as compared to the commonly used $1\ \Omega\text{cm}$ material.

A concept for the realisation of semitransparent crystalline silicon solar cells on CZ-silicon has been presented. A very

simple, industrially compatible process was developed and only six different process steps were necessary to reach cell efficiencies close to 10%.

Efficiencies exceeding 11% on this novel semitransparent monofacial crystalline silicon solar cells with a transmittance of 20% seem to be possible in the future when incorporating the above mentioned aspects in the redesigned solar cell process.

ACKNOWLEDGEMENTS

We like to thank M. Keil for technical assistance during solar cell processing. This work was supported by the German bmbf and *sunways* corporation, Konstanz, Germany.

LITERATURE

- [1] G.Willeke, P.Fath „The POWER silicon solar cell“ 12th European PVSEC, Amsterdam 1994
- [2] G.Willeke, P.Fath „Mechanical wafer engineering for semitransparent polycrystalline silicon solar cells“, Appl. Phys. Lett. **64** (10), 7 March 1994
- [3] G.Willeke, P.Fath, E.Bucher „Progress on the Power silicon solar cell“ 1st IEEE World Conference on PV Energy Conversion, Hawaii, 1994
- [4] R.Kühn, „Investigation of the effects of p/n-junctions bordering on the surface of silicon solar cells“, this conference
- [5] Simulation program of Andreas Tickart, University of Konstanz, Germany
- [6] „DessisTM“, ISE AG corporation, Zürich, Switzerland